EMBO reports

scientific report

RelA/p65 functions to maintain cellular senescence by regulating genomic stability and DNA repair

Jingxin Wang[1], Naduparambil K. Jacob[1,2], Katherine J. Ladner[1], Amer Beg[3], James D. Perko[1], Stephan M. Tanner[1], Sandya Liyanarachchi[1], Richard Fishel[1,2,4] & Denis C. Guttridge[1,2,4+]

[1]Human Cancer Genetics Program, and [2]Department of Molecular Virology, Immunology and Medical Genetics, The Ohio State University, Columbus, Ohio, USA, [3]Department of Interdisciplinary Oncology, H. Lee Moffitt Cancer Center and Research Institute at University of South Florida, Tampa, Florida, USA, and [4]Arthur G. James Comprehensive Cancer Center, The Ohio State University, Columbus, Ohio, USA

Nuclear factor (NF)-κB is a positive regulator of tumour development and progression, but how it functions in normal cells leading to oncogenesis is not clear. As cellular senescence has proven to be an intrinsic tumour suppressor mechanism that cells must overcome to establish deregulated growth, we used primary fibroblasts to follow NF-κB function in cells transitioning from senescence to subsequent immortalization. Our findings show that *RelA/p65*$^{-/-}$ murine fibroblasts immortalize at considerably faster rates than *RelA/p65*$^{+/+}$ cells. The ability of *RelA/p65*$^{-/-}$ fibroblasts to escape senescence earlier is due to their genomic instability, characterized by high frequencies of DNA mutations, gene deletions and gross chromosomal translocations. This increase in genomic instability is closely related to a compromised DNA repair that occurs in both murine *RelA/p65*$^{-/-}$ fibroblasts and tissues. Significantly, these results can also be duplicated in human fibroblasts lacking NF-κB. Altogether, our findings present a fresh perspective on the role of NF-κB as a tumour suppressor, which acts in pre-neoplastic cells to maintain cellular senescence by promoting DNA repair and genomic stability.

Keywords: NF-κB; senescence; genomic stability; DNA repair; tumour development

EMBO reports (2009) **10**, 1272–1278. doi:10.1038/embor.2009.197

INTRODUCTION

Nuclear factor (NF)-κB proteins are expressed in nearly all mammalian cells and function in vertebrates as dimers of five subunits: RelA or p65, c-Rel, RelB, p50 and p52. NF-κB is activated by many stimuli, including cytokines, oxidative stress, oncogenes and DNA damage (Hayden & Ghosh, 2004; Janssens & Tschopp, 2006; Wu & Miyamoto, 2007). This activation occurs through IκB kinase phosphorylation of IκB, leading to proteasome-dependent degradation of IκB and subsequent nuclear localization of p50/p65 (Hayden & Ghosh, 2004). Besides its functions in immune cells, a lot of evidence supports the fact that NF-κB participates in human disease. With respect to cancer, studies show that oncogenes, viral proteins and chromosomal alterations all contribute to deregulated NF-κB, which functions to promote cellular proliferation, angiogenesis and anti-apoptosis (Karin *et al*, 2002; Hayden & Ghosh, 2004; Courtois & Gilmore, 2006). However, compared with these pro-oncogenic activities, considerably less information is available about how NF-κB functions in pre-neoplastic cells before the initiation of oncogenesis.

Normal cells have limited proliferation potential and undergo cellular senescence in response to DNA damage, telomere attrition or oncogenic stress (Campisi & d'Adda di Fagagna, 2007). Senescence is a major obstacle that cells must overcome to gain uncontrolled proliferation (Braig *et al*, 2005; Chen *et al*, 2005), and loss of tumour suppressor activity facilitates the exit from senescence, thus increasing the likelihood of tumour development (Beausejour *et al*, 2003; Christophorou *et al*, 2006). To examine NF-κB in the initial stages of oncogenesis, we used mouse and human fibroblast senescence models. Our findings reveal an unexpected tumour suppressor activity for NF-κB, which functions in DNA repair to preserve genome integrity and the senescent state.

RESULTS AND DISCUSSION

Mouse embryonic fibroblasts (MEF) were extracted from *p65*$^{+/+}$ or *p65*$^{-/-}$ null embryos and subsequently analysed by a 3T3 protocol. Results showed that cells proliferated and entered senescence with comparable rates, as measured by cell counting, bromodeoxyuridine incorporation and senescence-associated β-galactosidase staining (supplementary Fig S1A–E online).

[1]Human Cancer Genetics Program, and [2]Department of Molecular Virology, Immunology and Medical Genetics, The Ohio State University, Columbus, Ohio 43210, USA
[3]Department of Interdisciplinary Oncology, H. Lee Moffitt Cancer Center and Research Institute at USF, Tampa, Florida 33612, USA
[4]Arthur G. James Comprehensive Cancer Center, The Ohio State University, Columbus, Ohio 43210, USA
[+]Corresponding author. Tel: +1 614 688 3137; Fax: +1 614 688 8675; E-mail: denis.guttridge@osumc.edu

Received 2 March 2009; revised 14 July 2009; accepted 15 July 2009; published online 25 September 2009

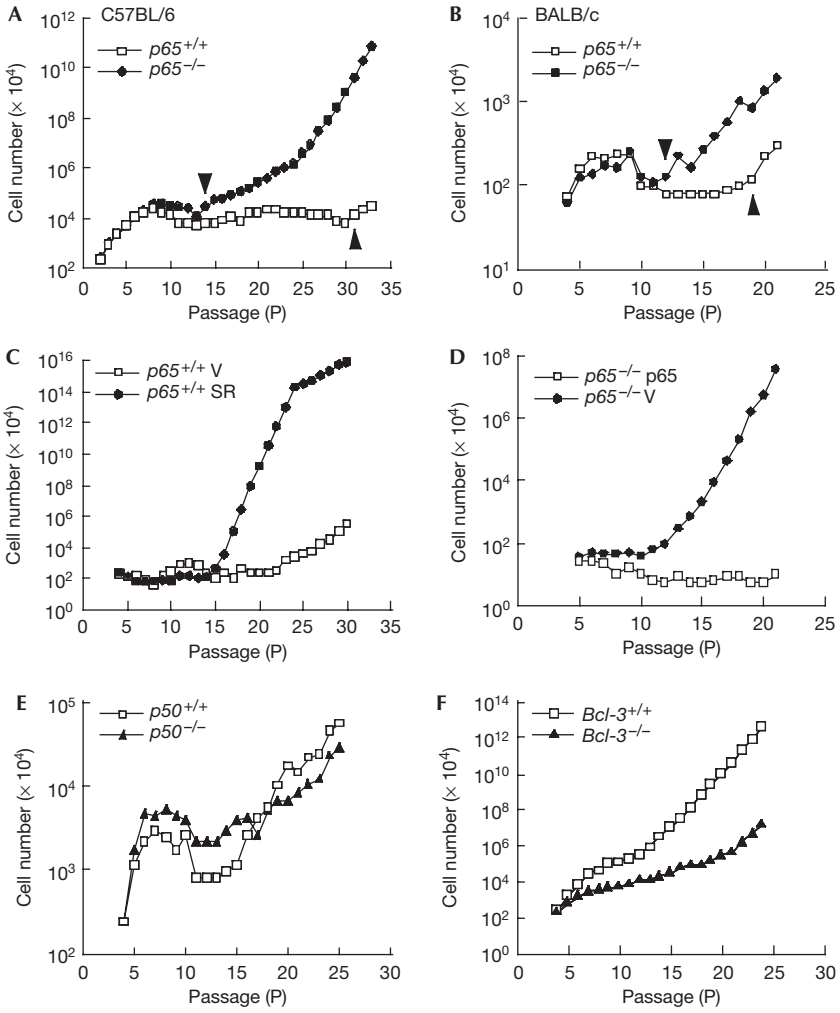

Fig 1 | *p65*$^{-/-}$ MEFs immortalize at a faster rate than wild type cells. (**A,B**) 3T3 analysis of *p65*$^{+/+}$ and *p65*$^{-/-}$ MEFs. Graph indicates the passage numbers at which C57BL/6 (**A**; $n=17$ pairs) or BALB/c (**B**; $n=3$ pairs) MEFs entered senescence and became immortalized. Arrowheads indicate passage numbers at which MEFs immortalize. (**C**) Immortalization of *p65*$^{+/+}$ MEFs expressing pBabepuro vector (V) or pBabeIκBα-SR (SR) by a 3T3 protocol ($n=3$). (**D**) Immortalization of *p65*$^{-/-}$ MEFs expressing pBabepuro vector (V) or pBabep65 (p65) ($n=3$). (**E,F**) *p50*$^{+/+}$ or *p50*$^{-/-}$ (**E**) and *Bcl-3*$^{+/+}$ or *Bcl-3*$^{-/-}$ (**F**) MEFs were prepared and passaged by a 3T3 protocol. MEF, mouse embryonic fibroblast.

However, unlike *p65*$^{+/+}$ cells, which remained senescent for at least 8–10 passages, *p65*$^{-/-}$ cells escaped senescence after as little as three passages (Fig 1A). Out of 17 pairs examined, 15 *p65*$^{-/-}$ lines immortalized 4–15 passages earlier than their *p65*$^{+/+}$ littermates. This early immortalization was independent of genetic background or the 3T3 protocol, as similar results were observed in *p65*$^{-/-}$ MEFs isolated from BALB/c mice, or passaged by a 3T9 method (Fig 1B; supplementary Fig S1F online). To confirm that this phenotype was nevertheless dependent on NF-κB, MEFs were stably infected with a retrovirus expressing the IκBα-SR (super repressor) inhibitor of NF-κB (supplementary Fig S2A online). In comparison with vector cells, IκBα-SR fibroblasts immortalized at an accelerated rate (Fig 1C). Moreover, reconstitution of p65 in *p65*$^{-/-}$ MEFs re-established a delay in immortalization (Fig 1D; supplementary Fig S2B online). This phenomenon seemed specific for p65 as *p50*$^{+/+}$ and *p50*$^{-/-}$ MEFs immortalized at comparable rates (Fig 1E), and MEFs null for the *Bcl-3* oncogene—which forms a transcriptional complex with p50 homodimers—required additional passages to undergo immortalization (Fig 1F). Altogether, these data indicate that p65 is required for maintaining a senescent state.

The evolution from normal to cancerous cells involves dynamic changes in the genome (Hanahan & Weinberg, 2000). To investigate the possibility that early immortalization of *p65*$^{-/-}$ MEFs might result from genetic alterations, chromosome counting was carried out on metaphase-arrested immortalized cells. Results showed that *p65*$^{-/-}$ MEFs contained a substantially higher number of chromosomes (Fig 2A). To see whether these genetic changes were a consequence of immortalization, chromosome counting was repeated in primary cells. Even as early as P4 when more than 90% of *p65*$^{+/+}$ cells are diploid, nearly 40% of *p65*$^{-/-}$ cells showed tetraploid chromosomes, and in a small, but significant portion of *p65*$^{-/-}$ cells (~5%, $P<0.05$), numbers reached noteworthy levels of 160–400 chromosomes per metaphase

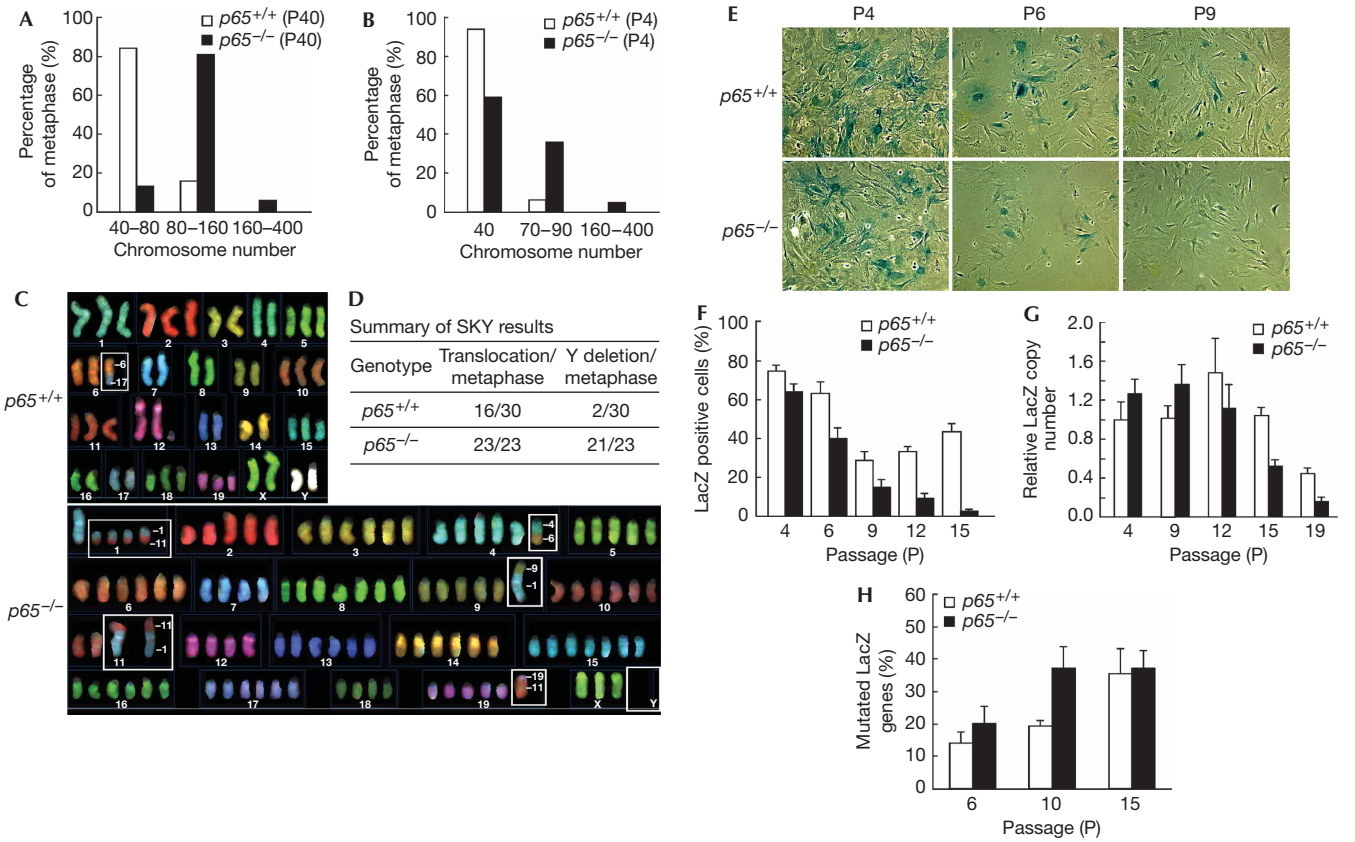

Fig 2 | p65 functions to regulate genomic stability. (**A**,**B**) Chromosomes were counted in (**A**) immortalized and (**B**) primary $p65^{+/+}$ and $p65^{-/-}$ MEFs from metaphase-arrested cells. (**C**,**D**) SKY of immortalized $p65^{+/+}$ and $p65^{-/-}$ cells at P42. (**E**,**F**) LacZ genomic stability assays ($n=3$) from primary $p65^{+/+}$ and $p65^{-/-}$ MEFs (P6, P9, P12, P15, $P<0.02$). (**G**) Quantitative RT–PCR of incorporated LacZ genes. (**H**) Early passage $p65+/+$ and $p65-/-$ MEFs were stably infected with pBabepuro–LacZ. The *LacZ* gene was amplified from DNA isolated from MEFs at indicated passages using high-fidelity PCR and then cloned into pBluescript SK+. Data show the percentage of white bacterial colonies grown on X-GAL LB agar plates. LB, Luria-Bertani; MEF, mouse embryonic fibroblast; RT–PCR, real-time PCR; SKY, spectrum karyotyping.

(Fig 2B; supplementary Fig S3A online). Spectrum karyotyping (SKY) was also carried out on immortalized MEFs to examine whether aneuploidy was accompanied with gross chromosome alterations. Out of 23 $p65^{-/-}$ metaphases studied, all contained $\geqslant 3$ chromosome translocations, whereas 21 out of 23 had $\geqslant 6$ chromosome translocations with total loss of chromosome Y (Fig 2C,D; supplementary Fig S3B online). By contrast, only 1–2 translocations occurred in 16 out of 30 metaphases in $p65^{+/+}$ cells, with 2 out of 30 cases showing the loss of chromosome Y. Furthermore, marker chromosomes that act as important indicators of genomic instability were only seen in $p65^{-/-}$ cells (supplementary Fig S3B,C online). These results suggested strongly that p65 functions as a regulator of genomic stability.

To quantitatively measure the differences in DNA integrity between $p65^{+/+}$ and $p65^{-/-}$ MEFs, we devised a LacZ genomic stability assay, in which the early loss of retroviral integrated LacZ expression indicates an unstable genome. Under these conditions, we observed that only 5% of $p65^{-/-}$ MEFs retained LacZ staining by P15, compared with 40% of $p65^{+/+}$ cells (Fig 2E,F). To determine whether these differences were due to LacZ deletion, genomic DNA was isolated and LacZ copy numbers were measured by quantitative real-time PCR (RT–PCR). We found that in late passages (P12–P19), *LacZ* gene copies were markedly decreased in $p65^{-/-}$ compared with $p65^{+/+}$ cells (Fig 2G), suggesting that gene deletion is enhanced in cells lacking p65. Given that this difference was not evident in earlier passages when LacZ staining was clearly reduced (Fig 2F, P6–P9, $P<0.02$), we investigated whether decreases in LacZ expression might also result from silencing mutations. Our results indicated that, although both $p65^{+/+}$ and $p65^{-/-}$ MEFs acquired mutations, the rate of these mutations was significantly higher in cells lacking p65 (Fig 2H, $P<0.005$). Taken together, these results infer that p65 functions in primary cells to maintain cellular senescence by regulating genomic stability.

Next, we investigated the mechanism by which p65 controls genomic stability. As DNA damage results from intrinsic and extrinsic factors that cause mutations and chromosomal aberrations in mammalian cells (Sancar *et al*, 2004), we considered that the absence of p65 might increase the level of reactive oxygen species leading to enhanced DNA damage. However, no differences in endogenous H_2O_2 or oxidative DNA damage were found between $p65^{+/+}$ and $p65^{-/-}$ MEFs (data not shown and supplementary Fig S4A,B online). Consequently, as increased abnormal chromosomal structures in $p65^{-/-}$ cells resembled the

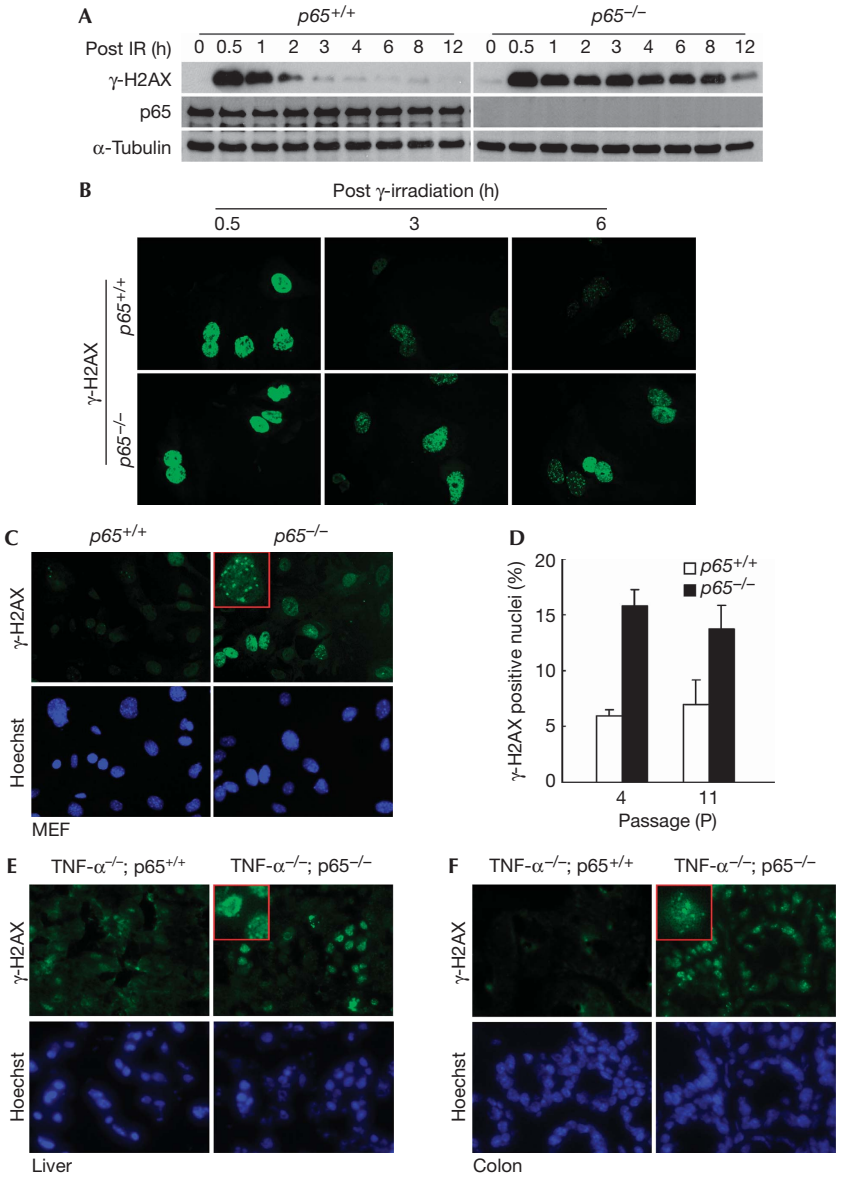

Fig 3 | *p65*$^{-/-}$ MEFs and tissues show defects in DNA repair. (**A**) P4–P6 MEFs were subjected to 8 Gy of IR. Whole-cell extracts were prepared at indicated time points and western blots were probed for γ-H2AX. (**B**) P4–P6 MEFs were treated with IR and recovery from DNA damage was analysed by using γ-H2AX immunofluorescence. (**C**) Basal levels of DNA damage in primary MEFs was analysed by γ-H2AX immunoflourescence. (**D**) Quantification of DNA-damage-positive nuclei in proliferating (P4) and senescent (P11) cells. Nuclei containing five or more brightly stained γ-H2AX foci were considered as positive. (**E,F**) Frozen sections from TNF-α;*p65*$^{+/+}$ or TNF-α;*p65*$^{-/-}$ livers and colons were stained for γ-H2AX. For each analysis, data are representative of three independent experiments. For quantitative analysis, data were derived from a minimum of 100 nuclei (**D**). Inserts represent γ-H2AX foci at × 1,000 magnification (**C,E,F**). Cells or sections were counterstained with Hoechst to visualize nuclei (**C,E,F**). IR, γ-irradiation; MEF, mouse embryonic fibroblast.

conditions of defective DNA repair (Gollin, 2005), such as in Fanconi anaemia (D'Andrea & Grompe, 2003), Bloom syndrome (German, 1993) and hereditary breast cancer syndromes (Scully & Livingston, 2000), we explored the potential link between p65 and DNA repair. Primary MEFs were, therefore, irradiated with graded doses of γ-rays and probed for γ-H2AX, a sensitive marker for the quantification of DNA damage and repair processes (Sedelnikova *et al*, 2002). Immunoblotting showed that γ-H2AX induction at 30 min was comparable between *p65*$^{+/+}$ and *p65*$^{-/-}$ cells, showing that p65 is not involved in ataxia telangiectasia mutated (ATM) activation of H2AX (supplementary Fig S5A online). However, whereas γ-H2AX decreased after 2 h of DNA damage in *p65*$^{+/+}$ cells, this signal persisted for 12 h in cells lacking p65 (Fig 3A), indicating that the recovery from DNA damage was compromised in *p65*$^{-/-}$ cells. Furthermore, immunostaining clearly showed that γ-H2AX foci persist in *p65*$^{-/-}$ nuclei after DNA damage (Fig 3B). This delayed recovery from DNA damage seemed to involve the DNA repair machinery, as the activation of

ATM and breast cancer 1 (BRCA1) also persisted in irradiated $p65^{-/-}$ cells (supplementary Fig S5C,D online). This regulation was not limited to irradiation as similar γ-H2AX results were seen in $p65^{-/-}$ cells treated with doxorubicin (supplementary Fig S5B online). Furthermore, accumulation of γ-H2AX occurred in proliferating (P4) and senescent (P11) MEFs, indicating that the DNA damage repair process is active in cells exposed to reactive oxygen stress under normal culture conditions. Significantly, this accumulation of damage foci was approximately three times higher in $p65^{-/-}$ MEFs compared with wild-type cells (Fig 3C,D; P4: $P<0.0005$; P11: $P<0.005$). To determine whether this regulation was relevant *in vivo*, γ-H2AX was monitored in tissues from $p65^{+/+}$ and $p65^{-/-}$ mice—maintained in a tumour necrosis factor-$\alpha^{-/-}$ background to rescue embryonic lethality (Doi *et al*, 1999). Consistent with MEFs, appreciably greater γ-H2AX-positive nuclei were seen in many $p65^{-/-}$ tissues, including liver, colon, spleen and kidney (Fig 3E,F; supplementary Fig S6A,B online). We reasoned that this basal γ-H2AX *in vivo* could be caused by inefficient repair of DNA damage derived from basal metabolite intermediates. Moreover, DNA repair was also visibly delayed in $p65^{-/-}$ tissues after sub-lethally irradiating $p65^{-/-}$ mice (supplementary Fig S6C,D online). These results strongly suggested that γ-H2AX signals persist in $p65^{-/-}$ tissues due to inefficient DNA repair.

MEFs senesce because of cumulative oxidative DNA damage in normal culture conditions (20% O_2), but can evade premature senescence when grown in physiological oxygen conditions (3% O_2; Parrinello *et al*, 2003). If inefficient DNA repair caused the early immortalization of $p65^{-/-}$ MEFs, then predictably eliminating the DNA damage that occurs in a 20% O_2 condition would also eliminate the need for repair, and thereby rescue the early immortalization phenotype. To test this prediction, we switched cells from a 20% to 3% O_2 condition, which effectively reduced the damage index from 1.8 to 0.3 in both $p65^{+/+}$ and $p65^{-/-}$ MEFs (Fig 4A). When cells were then forced into senescence with 8 Gy of γ-ray and maintained in 3% O_2 (supplementary Fig S7 online), all six pairs of $p65^{+/+}$ and $p65^{-/-}$ MEFs failed to become immortalized, even after 35 passages (>90 days; Fig 4B). However, when senescent MEFs cultured in 3% O_2 were switched back to 20% O_2, three out of four $p65^{-/-}$ MEF lines became immortalized, whereas none out of four $p65^{+/+}$ lines were able to escape senescence (Fig 4C). From these results, we concluded that defective DNA repair in $p65^{-/-}$ MEFs is likely to lead to accumulating genetic changes that facilitate the early exit from senescence.

Finally, we tested the relevance of our findings by repeating our analyses in human cells. Unlike MEFs, human cells are resistant to oxidative stress under 20% O_2 culture conditions and only undergo replicative senescence by telomere attrition (Sherr & DePinho, 2000). Thus, spontaneous immortalization is not seen in these cells without the reconstitution of mechanisms to maintain telomere length (Kiyono *et al*, 1998). Consistent with this idea, IκBα-SR expression in primary foreskin fibroblasts (HFs) was not sufficient for cells to escape senescence (data not shown). Thus, we repeated the experiment by sequentially expressing human telomerase reverse transcriptase (TERT) and IκBα-SR (supplementary Fig S8A,B online). Under these conditions, both vector (HF-TERT/V) and IκBα-SR (HF-TERT/SR) cells bypassed senescence and maintained their replicative potential for more than

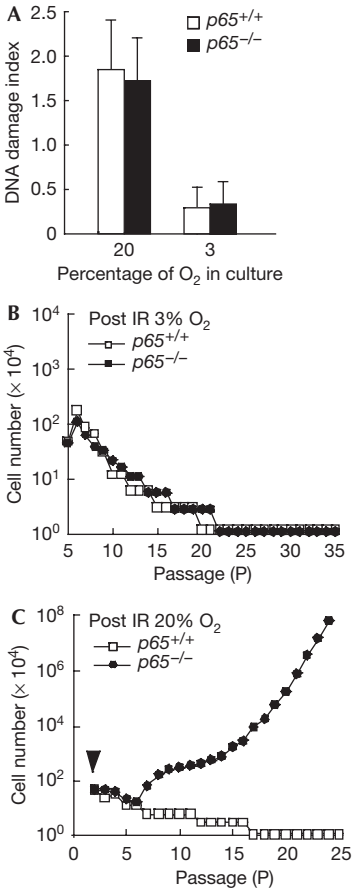

Fig 4 | Early immortalization of $p65^{-/-}$ MEFs is dependent on continuous DNA damage. (**A**) Oxidative DNA damage in $p65^{+/+}$ and $p65^{-/-}$ cells cultured under 20% O_2 or 3% O_2 was analysed by FLARE comet assay. Tail length and percentage of tail DNA contents were calculated using Cometscore software (TriTek Corporation). DNA damage index was derived from three independent experiments, with at least 50 nuclei counted per experiment. (**B**) $p65^{+/+}$ and $p65^{-/-}$ cells were cultured by a 3T3 method after IR-induced senescence under 3% O_2. Data represent experiments from six pairs of primary MEFs. (**C**) 3T3 analysis ($n=3$) of $p65^{+/+}$ or $p65^{-/-}$ MEFs after cells were induced to senesce with IR and switched from 3% to 20% O_2. Arrowhead indicates the passage at which cells were irradiated. IR, γ-irradiation; MEF, mouse embryonic fibroblast.

100 passages (data not shown). To induce senescence, cells were damaged for ten consecutive days with an empirically derived dose of H_2O_2 (supplementary information online). Similarly to $p65^{+/+}$ and $p65^{-/-}$ MEFs cultured in 3% O_2 after irradiation, both HF-TERT/V and HF-TERT/SR cells grown in 20% O_2 remained senescent for more than 50 weeks after the removal of H_2O_2 (supplementary Fig S8C online), owing to their resistance to oxidative stress. However, persistent intermittent treatment of senescent cells with H_2O_2 to produce repetitive DNA damage caused HF-TERT/SR, but not HF-TERT/V cells, to immortalize after only 16–20 weeks (Fig 5A). Significantly, out of four pairs of HF lines tested from two independent experiments, three HF-TERT/SR lines escaped senescence, of which two became permanently immortalized

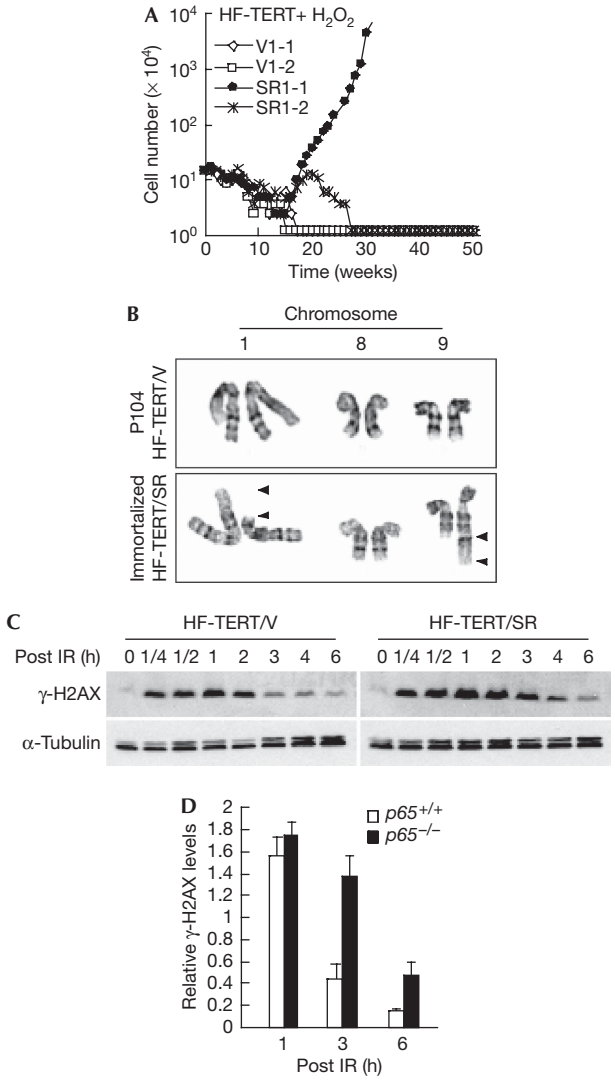

Fig 5 | p65 is required to maintain cellular senescence in HFs. (**A**) HFs were sequentially infected with retroviruses expressing human TERT and pBabepuro (HF-TERT/V) or pBabe-IκBα-SR (HF-TERT/SR) in a total of eight independent lines (supplementary Fig S8D online). Cells were treated with 400 μM H_2O_2 for 10 days to induce cellular senescence and subsequently immortalized by using intermittent H_2O_2 treatment. Cell numbers were determined on a weekly basis for 50 weeks. (**B**) Karyotyping results of immortalized HF from line HF-TERT/SR1-1. Chromosomes 1 and 9 are shown to indicate the unbalanced translocation event, whereas chromosome 8 is shown as a reference. Arrowheads indicate break points. (**C**) Western blot of γ-H2AX in proliferating (P35) HF-TERT/V and HF-TERT/SR cells following IR similar to that described in Fig 3A. (**D**) Expression levels of γ-H2AX at indicated time points in (**C**) were quantified by NIH image software from three independent experiments. HF, human fibroblast; IR, γ-irradiation; NIH, National Institutes of Health; SR, super repressor; TERT, telomerase reverse transcriptase.

(Fig 5A; supplementary Fig S8D online), whereas none out of four HF-TERT/V lines overcame senescence. In addition, HF-TERT/V cells maintained normal chromosome structures even after one year of continued passaging (P104). By contrast, HF-TERT/SR-immortalized cells contained a distinct t(1; 9) (p31.2; q34.3) chromosomal translocation (Fig 5B; supplementary Fig S8E online). Interestingly, the 9q34 region contains multiple tumour suppressor and tumour promoter genes, deletions, insertions or chromosomal translocations of which are linked with many human malignancies (supplementary Table 1 online). In addition, we also found that HF-TERT/SR cells showed a delayed recovery from DNA damage (Fig 5C,D). These results corroborate our findings in rodent cells that NF-κB maintains cellular senescence by regulating DNA repair and genome stability.

Taken together, our study adds to the current understanding of the biological function of NF-κB in cellular senescence. Previous studies carried out in human keratinocytes showed that forced expression of c-Rel was sufficient to induce senescence through an oxidative-stress-related mechanism (Bernard *et al*, 2004). Recent findings also support that the deacetylase silent mating type information regulation 2 homologue 6 (*S. cerevisiae*), inhibits senescence through direct repression of p65 (Kawahara *et al*, 2009). Furthermore, skin cells devoid of NF-κB activity were shown to exhibit deregulated growth correlating with impaired cell-cycle control (Seitz *et al*, 1998; Zhang *et al*, 2005). Although we were not able to observe overt changes in the cell cycle due to the absence of p65, our data showing that damaged $p65^{-/-}$ MEFs and human fibroblasts lacking NF-κB activity prematurely exit from senescence is consistent with the idea that NF-κB functions as a positive modulator of cellular senescence. How NF-κB contributes to senescence might be related to cell types that distinguish whether NF-κB initiates senescence, as seen in keratinocytes, or acts further downstream in DNA repair to maintain the senescent state.

As senescence is considered to be a major barrier for tumour development, our findings further reveal that NF-κB has a tumour suppressor activity relevant in the initial phases of oncogenesis. This idea is in agreement with several studies showing that disruption of NF-κB *in vivo* can stimulate tumour development (Dajee *et al*, 2003; Maeda *et al*, 2005; Luedde *et al*, 2007). Although not investigated, it would be interesting to determine in these respective models whether deletion of NF-κB might also give way to increased DNA damage as a result of compromised repair, thus leading to accumulated mutations and eventual tumour development. In the light of the overwhelming amount of evidence supporting the pro-oncogenic role of NF-κB, we favour the view (Perkins & Gilmore, 2006) that NF-κB has both tumour suppressor and tumour promoter functions, and how these functions manifest themselves during tumour development greatly depends on the genetic and epigenetic make-up of the cell. In pre-neoplastic cells undergoing stress-induced senescence, NF-κB would function as a tumour suppressor by contributing to DNA repair and genomic stability thus, maintaining cells in a senescent state. However, on acquiring sufficient genetic changes, activated oncogenes might tip the balance of NF-κB towards a tumour-promoting function that mediates cell survival, anti-differentiation and proliferation to facilitate the development and progression of tumours.

METHODS

Cell culture and 3T3 analysis. MEFs were isolated at day 13.5 post-coitus and cultured with Dulbecco's modified Eagle's

medium-H plus 10% fetal bovine serum. Immortalization of primary MEFs was carried out by trypsinizing and replating 3×10^5 (3T3 protocol) cells per 6 cm dish every three days.

LacZ genomic stability assay. Early passage primary MEFs were infected with pBabe–LacZ retrovirus. Cells were selected for three passages with 2 μg/ml puromycin and divided into three dishes for continuous passage without selection. From each passage, several cells were cultured overnight in duplicate and subsequently stained for β-GAL. For LacZ mutational analysis, infected cells were cultured under constant selection. DNA was extracted and the *LacZ* gene was amplified using PfuUltra (Stratagene, La Jolla, CA, USA) with primers listed in supplementary Table S2 online. The amplified *LacZ* gene was then cloned into pBluescript SK + in reverse orientation to the endogenous *LacZ* gene and transformed into bacteria *Escherichia coli*, DH5α. LB agar plates were prepared by spreading 40 μl of 20 mg/ml X-GAL and 40 μl of 100 mM isopropyl-β-D-thiogalactopyranoside.

Supplementary information is available at *EMBO reports* online (http://www.emboreports.org).

ACKNOWLEDGEMENTS

We thank E. Hertlein, M. Carathers, N. Bakkar and J.L. Chong for technical assistance during this study; J. Koeman for spectrum karyotyping analysis; and members of the Guttridge laboratory for discussions throughout the preparation of this paper. This study was supported by Up on the Roof and National Institutes of Health oncology fellowships to J.W., and by the Ohio State University Comprehensive Cancer Center.

CONFLICT OF INTEREST

The authors declare that they have no conflict of interest.

REFERENCES

Beausejour CM, Krtolica A, Galimi F, Narita M, Lowe SW, Yaswen P, Campisi J (2003) Reversal of human cellular senescence: roles of the p53 and p16 pathways. *EMBO J* **22:** 4212–4222

Bernard D, Gosselin K, Monte D, Vercamer C, Bouali F, Pourtier A, Vandenbunder B, Abbadie C (2004) Involvement of Rel/nuclear factor-kappaB transcription factors in keratinocyte senescence. *Cancer Res* **64:** 472–481

Braig M, Lee S, Loddenkemper C, Rudolph C, Peters AH, Schlegelberger B, Stein H, Dorken B, Jenuwein T, Schmitt CA (2005) Oncogene-induced senescence as an initial barrier in lymphoma development. *Nature* **436:** 660–665

Campisi J, d'Adda di Fagagna F (2007) Cellular senescence: when bad things happen to good cells. *Nat Rev Mol Cell Biol* **8:** 729–740

Chen Z *et al* (2005) Crucial role of p53-dependent cellular senescence in suppression of Pten-deficient tumorigenesis. *Nature* **436:** 725–730

Christophorou MA, Ringshausen I, Finch AJ, Swigart LB, Evan GI (2006) The pathological response to DNA damage does not contribute to p53-mediated tumour suppression. *Nature* **443:** 214–217

Courtois G, Gilmore TD (2006) Mutations in the NF-kappaB signaling pathway: implications for human disease. *Oncogene* **25:** 6831–6843

D'Andrea AD, Grompe M (2003) The Fanconi anaemia/BRCA pathway. *Nat Rev Cancer* **3:** 23–34

Dajee M *et al* (2003) NF-kappaB blockade and oncogenic Ras trigger invasive human epidermal neoplasia. *Nature* **421:** 639–643

Doi TS, Marino MW, Takahashi T, Yoshida T, Sakakura T, Old LJ, Obata Y (1999) Absence of tumor necrosis factor rescues RelA-deficient mice from embryonic lethality. *Proc Natl Acad Sci USA* **96:** 2994–2999

German J (1993) Bloom syndrome: a Mendelian prototype of somatic mutational disease. *Medicine (Baltimore)* **72:** 393–406

Gollin SM (2005) Mechanisms leading to chromosomal instability. *Semin Cancer Biol* **15:** 33–42

Hanahan D, Weinberg RA (2000) The hallmarks of cancer. *Cell* **100:** 57–70

Hayden MS, Ghosh S (2004) Signaling to NF-kappaB. *Genes Dev* **18:** 2195–2224

Janssens S, Tschopp J (2006) Signals from within: the DNA-damage-induced NF-kappaB response. *Cell Death Differ* **13:** 773–784

Karin M, Cao Y, Greten FR, Li ZW (2002) NF-kappaB in cancer: from innocent bystander to major culprit. *Nat Rev Cancer* **2:** 301–310

Kawahara TL *et al* (2009) SIRT6 links histone H3 lysine 9 deacetylation to NF-kappaB-dependent gene expression and organismal life span. *Cell* **136:** 62–74

Kiyono T, Foster SA, Koop JI, McDougall JK, Galloway DA, Klingelhutz AJ (1998) Both Rb/p16INK4a inactivation and telomerase activity are required to immortalize human epithelial cells. *Nature* **396:** 84–88

Luedde T, Beraza N, Kotsikoris V, van Loo G, Nenci A, De Vos R, Roskams T, Trautwein C, Pasparakis M (2007) Deletion of NEMO/IKKgamma in liver parenchymal cells causes steatohepatitis and hepatocellular carcinoma. *Cancer Cell* **11:** 119–132

Maeda S, Kamata H, Luo JL, Leffert H, Karin M (2005) IKKbeta couples hepatocyte death to cytokine-driven compensatory proliferation that promotes chemical hepatocarcinogenesis. *Cell* **121:** 977–990

Parrinello S, Samper E, Krtolica A, Goldstein J, Melov S, Campisi J (2003) Oxygen sensitivity severely limits the replicative lifespan of murine fibroblasts. *Nat Cell Biol* **5:** 741–747

Perkins ND, Gilmore TD (2006) Good cop, bad cop: the different faces of NF-kappaB. *Cell Death Differ* **13:** 759–772

Sancar A, Lindsey-Boltz LA, Unsal-Kacmaz K, Linn S (2004) Molecular mechanisms of mammalian DNA repair and the DNA damage checkpoints. *Annu Rev Biochem* **73:** 39–85

Scully R, Livingston DM (2000) In search of the tumour-suppressor functions of BRCA1 and BRCA2. *Nature* **408:** 429–432

Sedelnikova OA, Rogakou EP, Panyutin IG, Bonner WM (2002) Quantitative detection of (125)IdU-induced DNA double-strand breaks with gamma-H2AX antibody. *Radiat Res* **158:** 486–492

Seitz CS, Lin Q, Deng H, Khavari PA (1998) Alterations in NF-kappaB function in transgenic epithelial tissue demonstrate a growth inhibitory role for NF-kappaB. *Proc Natl Acad Sci USA* **95:** 2307–2312

Sherr CJ, DePinho RA (2000) Cellular senescence: mitotic clock or culture shock? *Cell* **102:** 407–410

Wu ZH, Miyamoto S (2007) Many faces of NF-kappaB signaling induced by genotoxic stress. *J Mol Med* **85:** 1187–1202

Zhang JY, Tao S, Kimmel R, Khavari PA (2005) CDK4 regulation by TNFR1 and JNK is required for NF-kappaB-mediated epidermal growth control. *J Cell Biol* **168:** 561–566